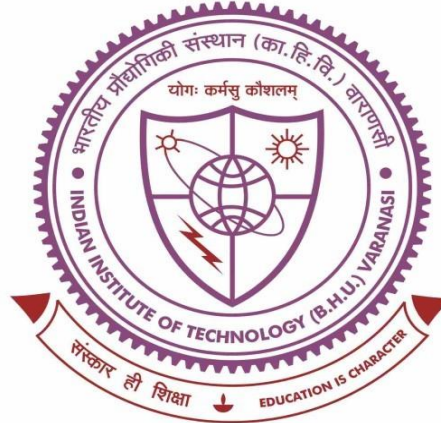


**NUMERICAL STUDY OF CONSOLIDATION  
BEHAVIOUR FOR SATURATED AND UNSATURATED  
SOILS**



**A Thesis**

Submitted for the Degree of  
***Doctor of Philosophy***

By  
**Amit Singh**

Under the supervision of  
**Dr. Manash Chakraborty**

**DEPARTMENT OF CIVIL ENGINEERING  
INDIAN INSTITUTE OF TECHNOLOGY  
BANARAS HINDU UNIVERSITY  
VARANASI-221005  
INDIA**

**18061502**

**2024**

## CERTIFICATE

It is certified that the work contained in the thesis titled “**NUMERICAL STUDY OF CONSOLIDATION BEHAVIOUR FOR SATURATED AND UNSATURATED SOILS**” has been carried out under my supervision and this work has not been submitted elsewhere for a degree.

It is further certified that the student has been fulfilled all the requirements of Comprehensive Examination, Candidacy, and State of the Art (SOTA) for the award of Ph.D degree.



**Dr. Manash Chakraborty**

**Supervisor**

**Assistant Professor**

**Dept. of Civil Engineering**

**IIT(BHU)**

**Varanasi, U.P, India-221005**

## DECLARATIONS BY THE CANDIDATE

I, **Amit Singh**, certify that the work embodied in this thesis is my own bonafide work and carried out by me under the supervision of **Dr. Manash Chakraborty** from **January 2019 to July 2024** at the **Department of Civil Engineering, IIT (BHU), Varanasi**. The matter embodied in this has not been submitted for the award of any other degree/diploma. I declare that I have faithfully acknowledged and given credits to the research workers wherever their works have been cited in my work in this thesis. I further declare that I have not wilfully copied any other's work, paragraphs, text, data, results, etc, reported in journals, books, magazines, reports dissertations, thesis, etc., or available at websites and included them in this thesis and cited as my own work.

Date:

Place: Varanasi

*Amit Singh*  
(Amit Singh)

## CERTIFICATE BY THE SUPERVISOR

It is certified that the above statement made by the student is correct to the best of my knowledge.

*Manash Chakraborty*  
**Dr. Manash Chakraborty**  
Supervisor  
Assistant Professor  
Dept. of Civil Engineering  
IIT (BHU)Varanasi,  
U.P, India-221005

*22.07.24*  
**Signature of Head of Department/Coordinator of School**  
**"SEAL OF THE DEPARTMENT/SCHOOL"**

दिभागस्य/HEAD  
आनपद अभियंत्रिणी विभाग  
Department of Civil Engineering  
भारतीय प्रौद्योगिकी संस्थान (IIT) (BHU)  
Institute of Technology (IIT) (BHU)  
Varanasi, U.P. 221005  
II

## **COPYRIGHT TRANSFER CERTIFICATE**

**Title of the Thesis: NUMERICAL STUDY OF CONSOLIDATION BEHAVIOUR FOR SATURATED AND UNSATURATED SOILS.**

**Name of the Student: Mr. Amit Singh**

### **Copyright Transfer**

The undersigned hereby assigns to the Indian Institute of Technology, (BHU), Varanasi, all rights under copyright that may exist in and for the above thesis for the award of the Doctor of Philosophy.

**Date:**

**Place: Varanasi**

*Amit Singh*  
(Amit Singh)

**Note:** However, the author may reproduce or authorize others to reproduce material extracted verbatim from the thesis or derivative of the thesis for the author's personal use provided that the source and the Institute's copyright notice are indicated.

# ACKNOWLEDGMENT

---

---

First and foremost, I would like to express my deepest gratitude to Lord Shiva for blessing me with countless opportunities, knowledge, and unwavering support, enabling me to complete this thesis successfully. Though my name appears on the cover, the accomplishment of this dissertation would not have been possible without the assistance and guidance of numerous individuals, to whom I owe my heartfelt appreciation.

I am immensely grateful to my supervisor, **Dr. Manash Chakraborty**, from the Civil Engineering Department at IIT (BHU), Varanasi, for his exceptional guidance, continuous monitoring, and unwavering encouragement throughout the entire duration of this research work. I am indebted to Dr. Manash Chakraborty for his invaluable inspiration and helpful recommendations, which significantly contributed to completing my research.

I extend my sincere appreciation to the members of my RPEC, Dr. Abhisek Mudgal as the internal expert and Dr. Debdas Ghosh as the external expert, for their valuable assistance, insightful suggestions, and constant encouragement during the entirety of my research work.

Furthermore, I would like to express my gratitude to Prof. Sasankasekhar Mandal, Head of the Department of Civil Engineering, Indian Institute of Technology (BHU), Varanasi, for providing the necessary facilities for my research. My heartfelt regards go to Prof. Arun Prasad, Dr. Bala Ramudu Paramkusam, Dr. Suresh Kumar, Dr. Supriya Mohanty, and all the faculty members of the Civil Engineering Department for their unconditional support throughout my academic journey.

I am also thankful to my friends and colleague, Dr. Manish Mandal, Mrs. Shivani Dhiriyan, Dr. Parul Rawat, Dr. Amit Kumar Ram, Mr. Abhay Kumar, Dr. Mohit Chaudhary, Mr. Vivek Wagh, Mr. Nirmal Prasad and my whole cricket team for their thought-provoking discussions, unwavering support, cooperation, and assistance in various ways.

In particular, I would like to express my heartfelt appreciation to some senior Dr. Nitesh Singh Bonal, Dr. Sourav Sarkar, Dr. Suryadev Prasad for their constant encouragement, love, and moral support. And special thanks to my junior Mr. Pushkar Nath Chaurasia who is very supportive in last phase of my PhD. I take immense pleasure in sharing the credit for my research work with all my teachers who have played a significant role at different stages of my academic career.

Lastly, I am eternally grateful to my entire family for their unwavering faith, patience, encouragement, blessings, and unconditional love. My deepest appreciation goes to my father and my mother for their steadfast motivation, belief in me, and continuous support. A special thanks to my special family for always holding my hand through the ups and downs, providing unwavering support and love.

I am sincerely grateful to each and every individual mentioned above, as well as those who have supported me in various ways, for their invaluable contributions to the completion of this thesis.

  
Amit Singh

# ABSTRACT

---

---

The mathematical model representing the classical Terzaghi's (1925) one-dimensional consolidation theory was developed on the premises of a few drastic idealizations. With the advancement in computational flexibilities and vast researches on soil mechanics, most of the involved assumptions in the conventional approach of settlement estimation appear inconsequential. The present thesis revisits Terzaghi's (1925) one-dimensional consolidation theory, from the following few perspectives: (a) initial condition associated with the load-imposed excess pore pressure, (b) boundary condition connected to the drainage boundaries, (c) governing differential equations related to the loading pattern, velocity-gradient relationship, stress-induced heterogeneities, and saturation states, and (d) coupling of the stress-deformation alongwith the pore pressure dissipation equation. The classical Terzaghi's one-dimensional linear parabolic diffusion equation is sufficiently modified and used for performing the consolidation analysis of saturated soil. The entire numerical analyses are conducted by using the Crank-Nicolson finite difference scheme

An attempt has been made to study the consolidation of homogeneous and two-layered soil by considering ten different spatial distributions of initial excess pore water pressure ( $u_0$ ) profiles. The variation of normalized pore pressure isochrones and the trend of the consolidating curves for different distributions of  $u_0$  are extensively evaluated and critically analyzed. A new approach has been developed to study the consolidation phenomenon through the locus of the maximum point of the isochrones.

Next, a study is conducted to understand the consequences of stress-dependent permeability and compressibility on the consolidation of inherently homogenous clays. The

importance of stress- and spatial-gradient of permeability in the consolidation analysis is established. Furthermore, permeability variation is integrated with non-Darcian flow models under ramp loading. The spatial and temporal permeability variation ( $k$ -isochrones) are also plotted to explain the variation in the consolidation curves.

In contrast to the traditional uncoupled consolidation, coupled methods, which integrate pore water pressure dissipation with soil deformation, provide more reliable solutions, especially for time-dependent loading and other complicated conditions. A detailed one-dimensional coupled consolidation is performed to investigate the combined influence of semipermeable drainage boundaries, non-Darcian fluid flow, and periodic loading. The non-Darcian flow is realized by employing the exponential and threshold gradient-based non-linear model. Traditionally, to simplify the numerical scheme, the hydraulic gradient in the exponential term is evaluated at the previous (known) time state, which converts the nonlinear equation into a linear equation. By adopting Newton-Raphson technique, an effort has been initiated to solve the actual nonlinear equation by computing the gradients at the current (unknown) time state.

The construction of geotechnical structures frequently occurs under partially saturated conditions. The unsaturated consolidation is governed by Fredlund and Rahardjo (1993)'s classical diffusion equations. The present thesis re-evaluates the impact of initial pore pressure condition, drainage boundaries, and velocity-gradient relations on the transient flow. To provide flexibility in the drainage, mixed drainage boundary conditions for the air and water phases are applied at the top and bottom boundary surfaces. A series of numerical experimentations are carried out. The results offer valuable insights for geotechnical engineering applications in various environmental conditions.



# CONTENTS

---

---

<b>ACKNOWLEDGEMENT.....</b>	<b>iv</b>
<b>ABSTRACT.....</b>	<b>vi</b>
<b>CONTENTS.....</b>	<b>ix</b>
<b>LIST OF FIGURES.....</b>	<b>xvii</b>
<b>LIST OF TABLES.....</b>	<b>xxv</b>
<b>LIST OF NOTATIONS.....</b>	<b>xxvii</b>
<b>LIST OF ABBREVIATIONS .....</b>	<b>xxvii</b>
<b>CHAPTER 1 Introduction.....</b>	<b>1</b>
1.1 GENERAL OVERVIEW.....	1
1.2 ASSUMPTIONS IN THE CLASSICAL CONSOLIDATION THEORY .....	2
1.2.1 Material properties .....	2
1.2.2 Flow properties .....	2
1.2.3 Drainage boundary.....	3
1.2.4 Loading characteristics .....	3
1.2.5 Geometric configuration .....	3
1.2.6 Mechanical response.....	3
1.3 BRIEF OVERVIEW OF CONSOLIDATION PROCESS.....	4
1.3.1 For saturated soil.....	4
1.3.2 For unsaturated soil.....	5
1.4 MOTIVATION AND OBJECTIVE OF THE WORK.....	7
1.5 ORGANIZATION OF THE THESIS.....	10
<b>CHAPTER 2 Literature Review.....</b>	<b>13</b>
2.1 INTRODUCTION.....	13
2.2 LITERATURES ON SATURATED CONSOLIDATION.....	13
2.2.1 Theories.....	13
2.2.2 Non-uniform initial excess pore water pressure.....	15
2.2.2.1 Singh (2005).....	15
2.2.2.2 Singh (2008).....	15

2.2.2.3 Singh and Swamee (2008).....	15
2.2.2.4 Lovisa et al. (2010).....	16
2.2.2.5 Lovisa et al. (2012).....	16
2.2.2.6 Lovisa and sivakugan (2014).....	16
2.2.2.7 Zhang et al (2015).....	17
2.2.3 Layered Soil.....	17
2.2.3.1 Chen et al. (2005).....	17
2.2.3.2 Mion et al. (2010).....	18
2.2.3.3 Kim and Mission (2011).....	18
2.2.3.4 Zhang et al. (2015).....	18
2.2.3.5 Yang et al. (2021).....	19
2.2.4 Varying permeability and compressibility.....	19
2.2.4.1 Schiffman (1958).....	19
2.2.4.2 Xie et al. (1995).....	19
2.2.4.3 Lekha et al. 2003.....	20
2.2.4.4 Zhuang et al. (2005).....	20
2.2.4.5 Ying-chun et al. (2005).....	20
2.2.4.6 Abbasi et al. (2007).....	21
2.2.4.7 Toufigh and Ouria (2009).....	21
2.2.5 Non darcian flow.....	22
2.2.5.1 Elnaggar et al. (1973).....	22
2.2.5.2 Ing and Xiaoyan (2002).....	22
2.2.5.3 Zhao and Gong (2019).....	22
2.2.5.4 Zong et al. (2021).....	23
2.2.6 Time dependent loading.....	23
2.2.6.1 Schiffman (1958).....	23
2.2.6.2 Wilson and Elgohary (1974).....	24
2.2.6.3 Baligh and Levadoux (1978).....	24
2.2.6.4 Xie and Pan (1995).....	24
2.2.6.5 Conte and Troncone (2006).....	25
2.2.6.6 Herrmann and Gendy (2014).....	25
2.2.6.8 Chai et al. (2022).....	26
2.2.6.9 Satwik and Chakraborty (2022).....	26
2.2.7 Coupled consolidation.....	27
2.2.7.1 Lewis et al. (1991).....	27

2.2.7.2 Huang et al. (2010).....	27
2.2.7.3 Osman (2010).....	28
2.2.7.5 Deng et al (2016).....	28
2.2.7.6 Baqersad et al. (2016).....	28
2.3 LITERATURES ON UNSATURATED CONSOLIDATION.....	29
2.3.1 Theories.....	29
2.3.2 Non- uniform initial excess pore pressures.....	30
2.3.2.1 Zhou and Zhao (2014).....	30
2.3.2.2 Zhao et al. (2014).....	30
2.3.3 Impeded boundary conditions.....	31
2.3.3.1 Wang et al. (2017a).....	31
2.3.3.2 Wang et al. (2017b).....	31
2.3.3.3 Wang et al. (2017c).....	31
2.3.3.4 Zhao et al. (2020).....	32
2.3.3.5 Zhou et al. (2021).....	32
2.3.3.6 Huang et al. (2021).....	32
2.4 SUMMARY.....	33

## **CHAPTER 3 Effect of Initial Excess Pore Water Pressure on Saturated Consolidation of Homogeneous/Layered Soil.....35**

3.1 INTRODUCTION.....	35
3.2 ASSUMED DISTRIBUTION OF INITIAL EXCESS PORE WATER PRESSURE.....	38
3.3 DEFINITION OF THE COMPUTED PARAMETERS.....	42
3.3.1 Isochrones.....	42
3.3.2 Consolidating curves ( $U_{avg}$ versus $T_v$ relationship).....	42
3.3.3 $u_{max}$ paths.....	42
3.4 HOMOGENEOUS SOIL.....	43
3.4.1 Problem Statement.....	43
3.4.2 Mathematical formulations.....	43
3.4.3 Solution Strategy.....	44
3.4.4 Results and Discussions.....	46
3.4.4.1 Isochrones and $u_{max}$ path for PTPB.....	46
3.4.4.2 Isochrones and $u_{max}$ path for PTIB.....	47
3.4.4.3 $U_{avg}$ versus $T_v$ curves for PTPB and PTIB.....	49

3.5 LAYERED SOIL.....	55
3.5.1 Problem Statement.....	55
3.5.2 NUMERICAL SCHEME.....	55
3.5.3 RESULTS AND DISCUSSIONS.....	57
3.5.3.1 Isochrones.....	57
3.5.3.2 $u_{max}$ path.....	59
3.5.3.3 $U_{avg}$ versus normalized time.....	59
3.5.3.4 Rate of dissipation with time.....	68
3.6 VALIDATION.....	73
3.7 SUMMARY.....	77

**CHAPTER 4 Effect of Stress-Dependent Permeability, Ramp Loading, and Non-Darcian Flow on Saturated Consolidation.....79**

4.1 INTRODUCTION.....	79
4.2 INVESTIGATING THE EFFECT OF QUASI AND TOTAL PERMEABILITY VARIATION.....	81
4.2.1 Problem Statement.....	81
4.2.1.1 Stress-Dependent Characteristics.....	81
4.2.2 Forms of the governing differential equations (GDE) .....	83
4.2.3 Numerical Scheme.....	85
4.2.4 Results and Discussions.....	86
4.2.4.1 Influence of $C/M$ on consolidation behaviour.....	87
4.2.4.2 Effect of $q$ on consolidation behaviour.....	90
4.3 IMPACT OF NON-DARCIAN FLOW RULE AND RAMP LOADING.....	93
4.3.1 Problem Statement.....	93
4.3.1.1 Non-linear flow Model and Stress-Dependent Characteristics.....	94
4.3.2 Formulations and Solution Strategy.....	94
4.3.3 Results and Discussions.....	98
4.3.3.1 Effect of Model Parameters and Construction Time.....	99
4.3.3.2 Effect of $A$ and $B$ Parameters on Permeability and Rate of Consolidation.....	102
4.3.3.3 Effect of $M$ and $C_c$ Parameters on Permeability and Rate of Consolidation.....	103
4.3.3.4 Effect of Various Parameters on the $u$ -Isochrones.....	106
4.4 VALIDATION OF RESULTS.....	115

4.5 SUMMARY.....	115
------------------	-----

**CHAPTER 5 Combined Effect of Cyclic Loading, Impeded Boundary Conditions and Non- Darcian Flow on Saturated Consolidation .....119**

5.1 INTRODUCTION.....	119
5.2 PROBLEM STATEMENT.....	123
5.3 NUMERICAL ANALYSIS.....	126
5.4 RESULTS AND DISCUSSIONS.....	127
5.4.1 Constant loading.....	127
5.4.2 Cyclic loading.....	129
5.5 SUMMARY.....	149

**CHAPTER 6 Simulating Non-Linear Flow by using Newton-Raphson Technique.....151**

6.1 INTRODUCTION.....	151
6.2 FORMULATIONS AND ANALYSIS.....	152
6.2.1 Crank Nicolson Implicit (CNI) Scheme:.....	153
6.2.1.1 Conventional Approach -- Method A1: Considering $t_m = t$ (i.e. previous time step).....	153
6.2.1.2 Modified Approach -- Method A2: Considering $t_m = t + \Delta t$ (i.e. current time step).....	153
6.2.2 Barakat–Clark (BKC) Method.....	155
6.2.2.1 Conventional Approach -- Method B1: Considering $t_m = t$ (i.e. previous time step).....	155
6.2.2.2 Modified Approach-- Method B2: Considering $t_m = t + \Delta t$ (i.e. current time step).....	155
6.3 NUMERICAL VERIFICATION.....	159
6.3.1 Problem Statement.....	159
6.4 RESULTS AND INTERPRETATIONS.....	159
6.5 VERIFICATION.....	162
6.6 SUMMARY.....	168

**CHAPTER 7 Effect Of Initial Excess Pore Pressures on Unsaturated Consolidation.....169**

7.1 INTRODUCTION.....	169
-----------------------	-----

7.2 PROBLEM STATEMENT.....	171
7.2.1 Assumptions Involved.....	173
7.2.2 Numerical Formulations.....	175
7.2.3 Solution Strategy.....	176
7.3 RESULTS AND DISCUSSION.....	176
7.3.1 Development of $u_{w0}$ and $u_{a0}$ .....	177
7.3.2 Isochrones and $u_{max}$ path.....	177
7.3.3 $U_{avg}$ versus time.....	180
7.3.4 Variation of pore pressure with time at different height.....	184
7.3.5 Rate of dissipation with time.....	185
7.4 VALIDATION.....	193
7.5 SUMMARY.....	193

**CHAPTER 8 Combined Effect of Non-Darcian Flow and Semi-Permeable Drainage Boundaries on Unsaturated Consolidation .....195**

8.1 INTRODUCTION.....	195
8.2 PROBLEM STATEMENT.....	196
8.3 NUMERICAL ANALYSIS.....	199
8.4 RESULT AND DISCUSSION.....	201
8.4.1 Dissipation of $u_{w0}$ and $u_{a0}$ .....	201
8.5 VERIFICATION.....	217
8.6 SUMMARY.....	220

**CHAPTER 9 Conclusions and Future Recommendations.....221**

9.1 CONCLUSION.....	221
9.2 LIMITATION AND SCOPE FOR FURURE WORK.....	225

**References.....227**

**Appendix A: Terzaghi’s (1925) diffusion equation and its discretization .....244**

**Appendix B: Construction and discretization of the GDEs considering stress dependencies, nonlinear flow, and ramp loading .....246**

<b>Appendix C: Modification and discretization of the coupled consolidation equation considering non-Darcian flow, periodic loading, and semi-permeable drainage boundaries.....</b>	<b>253</b>
<b>Appendix D: Forms of the coefficient and Jacobian matrices and the vectors for different methods.....</b>	<b>256</b>
<b>Appendix E: Derivation and discretization of the GDEs representing unsaturated consolidation .....</b>	<b>261</b>
<b>Appendix F: Modifications of the unsaturated GDEs to instill flexible drainage, and nonlinear flow.....</b>	<b>269</b>
<b>List of Publications.....</b>	<b>273</b>



## LIST OF FIGURES

<b>Fig. 3.1</b>	Various shapes of the assumed $u_0$ distribution: (a) Parabolic, (b) Triangular, (c and d) Trapezoidal, (e) Sine, (f) Cosine, (g) Half Sine Decreasing, (h) Half Sine Increasing, (i) Skewed, (j) Arched.	41
<b>Fig. 3.2</b>	Homogeneous consolidating stratum subjected to strip loading along with the finite difference discretization	44
<b>Fig. 3.3</b>	Isochrones and $u_{max}$ path for PTPB consolidating layer subjected to various $u_0$ loading	48
<b>Fig. 3.4</b>	$u_{max}$ path for PTPB consolidating layer for various $u_0$ loadings and the corresponding associated variables	49
<b>Fig. 3.5</b>	Isochrones and $u_{max}$ path for PTIB consolidating layer subjected to various $u_0$ loading	51
<b>Fig. 3.6</b>	$u_{max}$ path for PTIB consolidating layer for various $u_0$ loadings and the corresponding associated variable	52
<b>Fig. 3.7</b>	$U_{avg}$ versus $T_v$ curves for the consolidating layer subjected to two-way drainage	53
<b>Fig. 3.8</b>	$U_{avg}$ versus $T_v$ curves for the consolidating layer subjected to one-way drainage	54
<b>Fig. 3.9</b>	Two-layered consolidating stratum subjected to strip loading along with the finite difference discretization	56
<b>Fig. 3.10</b>	Corresponding to various initial excess PWP distributions, the variation of normalized isochrones for different $k_1/k_2$ ratios having $m_{v1}/m_{v2} = 1$ , $h_1/H = 0.3$ and subjected to two-way drainage	60
<b>Fig. 3.11</b>	Corresponding to various initial excess PWP distributions, the variation of normalized isochrones for different $m_{v1}/m_{v2}$ ratios having $k_1/k_2 = 1$ , $h_1/H = 0.3$ and subjected to two-way drainage	61
<b>Fig. 3.12</b>	Corresponding to various initial excess PWP distributions, the variation of normalized isochrones for different $h_1/H$ ratios having $k_1/k_2 = 1$ , $m_{v1}/m_{v2} = 10$ and subjected to two-way drainage	62

<b>Fig. 3.13</b>	Corresponding to various initial excess PWP distributions, the variation of normalized isochrones for different $k_1/k_2$ ratios having $m_{v1}/m_{v2} = 1$ , $h_1/H = 0.3$ and subjected to one-way drainage	63
<b>Fig. 3.14</b>	Corresponding to various initial excess PWP distributions, the variation of normalized isochrones for different $m_{v1}/m_{v2}$ ratios having $k_1/k_2 = 1$ , $h_1/H = 0.3$ and subjected to one-way drainage	64
<b>Fig. 3.15</b>	Corresponding to various initial excess PWP distributions, the variation of normalized isochrones for different $h_1/H$ ratios having $k_1/k_2 = 1$ , $m_{v1}/m_{v2} = 10$ and subjected to one-way drainage	65
<b>Fig. 3.16</b>	Variation of $u_{max}$ path by changing the controlling parameters of four $u_0$ distributions: (a) Case B, (b) Case I, (b) Case C, and, (b) Case D	67
<b>Fig. 3.17</b>	Corresponding to various initial excess PWP distributions, the variation of $U_{avg}$ with respect to normalized time for different $k_1/k_2$ ratios having $m_{v1}/m_{v2} = 1$ , $h_1/H = 0.3$ and subjected to two-way drainage	69
<b>Fig. 3.18</b>	Corresponding to various initial excess PWP distributions, the variation of $U_{avg}$ with respect to normalized time for different $m_{v1}/m_{v2}$ and $h_1/H$ ratios having $k_1/k_2 = 1$ , and subjected to two-way drainage	70
<b>Fig. 3.19</b>	Corresponding to various initial excess PWP distributions, the variation of $U_{avg}$ with respect to normalized time for different $k_1/k_2$ ratios having $m_{v1}/m_{v2} = 1$ , $h_1/H = 0.3$ and subjected to one-way drainage	71
<b>Fig. 3.20</b>	Corresponding to various initial excess PWP distributions, the variation of $U_{avg}$ with respect to normalized time for different $m_{v1}/m_{v2}$ and $h_1/H$ ratios having $k_1/k_2 = 1$ , and subjected to one-way drainage	72
<b>Fig. 3.21</b>	Variation of $RDR$ with respect to normalized time for different combinations of $k_1/k_2$ ( $r$ ) and $m_{v1}/m_{v2}$ ( $p$ ), corresponding to $h_1/H=0.3$ , and subjected to PTPB drainage conditions and various $u_0$ loadings	74
<b>Fig. 3.22</b>	Variation of $RDR$ with respect to normalized time for different combinations of $k_1/k_2$ ( $r$ ) and $m_{v1}/m_{v2}$ ( $p$ ), corresponding to $h_1/H=0.3$ , and subjected to PTIB drainage conditions and various $u_0$ loadings	75
<b>Fig. 3.23</b>	Comparisons of the present solutions with the solutions provided for (a) homogenous soil (Lambe and Whitman, 1969) and (b) layered soil (Luscher, 1965)	77

<b>Fig. 4.1</b>	(a) A schematic diagram of the problem statement, ramp loading applied (b) impact of various soil parameter on stress-dependent permeability.	82
<b>Fig. 4.2</b>	Relation between $e\text{-log}\sigma'\text{-log}k$ on logarithmic scale with (a) variation of $M$ and $B$ (b) variation of $C_c$ and $A$ .	86
<b>Fig 4.3</b>	Flow chart of the steps for consolidation	88
<b>Fig. 4.4</b>	Normalised isochrones for (a) PTPB condition (b) PTIB condition at $T_n=0.2$	89
<b>Fig. 4.5</b>	$U_{avg}$ vs $t_n$ for (a) PTPB condition (b) PTIB condition	89
<b>Fig. 4.6</b>	$u/u_0$ vs $T_n$ at mid-depth for (a) PTPB condition (b) PTIB condition	91
<b>Fig. 4.7</b>	Effect of loading for (a) $C_c/M = 0.5$ in PTPB drainage condition (b) $C_c/M$ $=1.5$ in PTPB drainage condition (c) $C_c/M = 0.5$ in PTIB drainage condition (d) $C_c/M = 1.5$ in PTIB drainage condition	91
<b>Fig. 4.8</b>	Effect of loading on $C_n/X_1$ for (a) $C_c/M = 0.5$ in PTPB drainage condition (b) $C_c/M = 1.5$ in PTPB drainage condition (c) $C_c/M = 0.5$ in PTIB drainage condition (d) $C_c/M = 1.5$ in PTIB drainage condition	92
<b>Fig. 4.9</b>	(a) Impact of various non-Darcian flow model parameter on normalized minimum permeability (b) ramp loading	95
<b>Fig. 4.10</b>	The nonlinear variation of flow velocity with hydraulic gradient with the parameter variation and different permeability	95
<b>Fig 4.11</b>	Consolidating curves for PTPB at three different construction time ( $t_c$ ), namely 0.0, 0.05, and 0.15 that corresponds to various model parameters.	104
<b>Fig. 4.12</b>	Consolidating curves for PTIB at three different construction time ( $t_c$ ), namely 0.0, 0.05, and 0.15 that corresponds to various model parameters.	105
<b>Fig. 4.13</b>	$k$ -isochrones graph for (a) $A$ variation in PTPB (b) $B$ variation IN PTPB (c) $A$ variation in PTIB (d) $B$ variation in PTIB	109
<b>Fig. 4.14</b>	Consolidation curve depicting variation of $C_c$ and $M$ in (a) ramp loading PTPB (b) ramp loading PTIB (c) constant loading in PTPB (d) constant load in PTIB	110
<b>Fig. 4.15</b>	$k$ -isochrones graph for (a) $C_c$ variation in PTPB (b) $M$ variation IN PTPB (c) $C_c$ variation in PTIB (d) $M$ variation IN PTIB	111
<b>Fig. 4.16</b>	Consolidation curve depicting variation of $C_c$ and $M$ in (a) ramp loading PTPB (b) ramp loading PTIB (c) constant loading in PTPB (d) constant load in PTIB	112

<b>Fig. 4.17</b>	Isochrones for Ramp ( $t_c = 0.05$ ) and constant load ( $t_c = 0$ ) in PTPB at time 32.40 days and 46.30 days with $C_c$ and $M$ variations	113
<b>Fig. 4.18</b>	Isochrones for Ramp ( $t_c = 0.05$ ) and constant load ( $t_c = 0$ ) in PTIB at time 32.40 days and 173 days with $C_c$ and $M$ variation	114
<b>Fig 4.19</b>	Comparisons of the present solutions with the solutions provided for (a) Abbasiet al. 2006, (b) and (c) Li et al. 2018, (d) and (e) Xie et al. 2012	116
<b>Fig 5.1</b>	Schematic representation of the chosen (a) clay layer bounded by the semi-impermeable boundaries, and (b) applied periodic loading	126
<b>Fig 5.2</b>	Impact of non-Darcian parameters on normalized isochrones corresponding to asymmetric drainage ( $R_T = \infty$ , $R_B = 10$ ) and constant loading	130
<b>Fig 5.3</b>	Impact of non-Darcian parameters on consolidation curves corresponding to symmetric drainage ( $R_T = R_B = \infty$ ) and constant loading.	131
<b>Fig 5.4</b>	Impact of non-Darcian parameters on settlement curves corresponding to symmetric drainage ( $R_T = R_B = \infty$ ) and constant loading.	132
<b>Fig 5.5</b>	Impact of non-Darcian and asymmetric boundary conditions on the consolidation curves for the chosen periodic loadings: (a-c) TL, (d-f) TRL, and (g-i) RL.	135
<b>Fig 5.6</b>	Impact of non-Darcian and asymmetric boundary conditions on the settlement curves for the chosen periodic loadings: (a-c) TL, (d-f) TRL, and (g-i) RL	136
<b>Fig 5.7</b>	Impact of non-Darcian parameters on the PWP profiles at three different locations ( $h/H = 0.2, 0.5$ and $0.8$ ) subjected to TL, $R_T = \infty$ , and $R_B$ equals to (a-c) $\infty$ , (d-f) 5, (g-i) 0.	138
<b>Fig 5.8</b>	The consolidation curves subjected to nonlinear flow, different symmetric boundaries ( $R=10, 5$ , and $1$ ), and periodic loadings: (a-c) TL, (d-f) TRL, and (g-i) RL.	139
<b>Fig 5.9</b>	The normalized settlement curves subjected to nonlinear flow, different symmetric boundaries ( $R=10, 5$ , and $1$ ), and periodic loadings: (a-c) TL, (d-f) TRL, and (g-i) RL.	140

<b>Fig 5.10</b>	The consolidation curves subjected to different loadings (a-c) TL, (d-f) TRL, and (g-i) RL with different cycle times ( $T_0$ ): (a,d,g) $10^7$ s, (b,e,h) $5 \times 10^7$ s, and (c,f,i) $10^8$ s.	142
<b>Fig 5.11</b>	The settlement curves subjected to different loadings (a-c) TL, (d-f) TRL, and (g-i) RL with different cycle times ( $T_0$ ): (a,d,g) $10^7$ s, (b,e,h) $5 \times 10^7$ s, and (c,f,i) $10^8$ s.	143
<b>Fig 5.12</b>	Combined impact of $\eta$ and $R_B$ on the range of elastic deformation ( $D_u$ ) for Darcian and non-Darcian flow corresponding to: (a) TL, (b)TRL, and (c) RL.	145
<b>Fig 5.13</b>	Combined impact of symmetric boundary condition and $t_0$ on range of elastic deformation ( $D_u$ ) for Darcian and non-Darcian flow for the trapezoidal loading.	146
<b>Fig 5.14</b>	The variation of normalized isochrones at different loading positions of the (a,d) TL, (b,e) TRL, and (c,f) RL periodic loadings.	147
<b>Fig 5.15</b>	The variation of normalized settlement at different loading positions of the (a,d) TL, (b,e) TRL, and (c,f) RL periodic loadings.	148
<b>Fig. 6.1.</b>	Pictorial representation of the time marching scheme using the (a) conventional approach (Method A1/B1) and (b) modified approach (Method A2/B2).	154
<b>Fig 6.2</b>	Comparisons of the normalized isochrones for different $\lambda$ and obtained from different finite difference schemes, namely, (a), (c) BKC and (b), (d) CNI	160
<b>Fig. 6.3</b>	Normalized isochrones for PTPB plotted at two different time and correspond to various model parameters and two different construction time factors ( $T_{vc}$ ), namely, 0.01 and 0.1.	163
<b>Fig. 6.4</b>	Normalized isochrones for PTIB plotted at two different time and correspond to various model parameters and two different construction time factors ( $T_{vc}$ ), namely, 0.01 and 0.1	164
<b>Fig. 6.5</b>	Consolidating curves for PTPB correspond to various model parameters and three different construction time factors ( $T_{vc}$ ), namely, 0.00, 0.01, and 0.1.	165

<b>Fig. 6.6</b>	Consolidating curves for PTIB correspond to various model parameters and three different construction time factors ( $T_{vc}$ ), namely, 0.00, 0.01, and 0.1.	166
<b>Fig.6.7</b>	Comparison of the present numerical solutions with the numerical solutions presented by Xie et al. 2012.	167
<b>Fig. 7.1.</b>	(a) Schematic diagram of the unsaturated consolidation process (b) meaning of compressibility parameters (c) schema of updating $u_{w(i)}$ and $u_{a(i)}$ .	172
<b>Fig. 7.2</b>	Variation of the initial excess pore water and pore air pressures with respect to saturation, porosity, and corresponding to various compressibility parameters, namely, (a) initial, (b) $5 \times m_{1k}^{si}$ , (c) $2 \times m_2^{si}$ , (d) $2 \times m_2^{wi}$ ; here, initial set indicates $m_{1k}^{si} = -2.5a, m_{1k}^{wi} = -0.5a, m_2^{si} = -a, m_2^{wi} = -2a$ with $a=10^{-4}$ and the other compressibility parameters in b, c, and d are the same.	178
<b>Fig. 7.3</b>	Spatial distributions of $u_j$ (isochrones) and $u_{jmax}$ path for PTIB and corresponding to the following $u_{j0}$ distributions:(a) uniform (b) sine (c) and (d) half sine increasing and decreasing (e) mid angle triangular (f) parabolic (g) and (h) trapezoidal (i) arched (j) skewed	181
<b>Fig. 7.4</b>	Spatial distributions of $u_j$ (isochrones) and $u_{jmax}$ path for PTIB and corresponding to the following $u_{j0}$ distributions:(a) uniform (b) sine (c) and (d) half sine increasing and decreasing (e) mid angle triangular (f) parabolic (g) and (h) trapezoidal (i) arched (j) skewed	182
<b>Fig. 7.5</b>	Consolidation curve corresponding for various $u_{j0}$ distributions subjected to two way drainage.	186
<b>Fig. 7.6</b>	Consolidation curve corresponding for various $u_{j0}$ distributions subjected to one-way drainage.	187
<b>Fig. 7.7</b>	Variation of normalized pore pressure with time at different depth (2m, 5m and 8m) subjected to PTPB boundary condition.	188
<b>Fig. 7.8</b>	Variation of normalized pore pressure with time at different depth (2m, 5m and 8m) subjected to PTIB boundary condition..	189
<b>Fig. 7.9</b>	$RDR_j$ curve for corresponding to various $u_{j0}$ distribution curve for PTPB boundary condition.	190

- Fig. 7.10**  $RDR_j$  curve for corresponding to various  $u_{j0}$  distribution curve for PTIB boundary condition. 191
- Fig. 7.11** The verifications of the present solutions on the basis of normalized isochrones with Zhou et al (2013). 192
- Fig. 8.1** Schematic representation of the chosen consolidating layer bounded by the semi-impermeable membranes. 197
- Fig. 8.2** The normalized pore pressure isochrones (Darcian and non-Darcian) with two asymmetric semi-permeable boundaries ( $R_T=200$ ,  $R_B=10$  and  $R_T=20$ ,  $R_B=5$ ) corresponding to relatively (a-c) early stage of consolidation ( $t=2.5 \times 10^6$ sec) with  $k_{ws}/k_{as}$  equals to: (a) 0.1, (b) 1, (c) 10, and (d-f) later stage of consolidation ( $t \gtrsim 10^8$ sec) with  $k_{ws}/k_{as}$  equals to: (d) 0.01, (e) 0.1, and (f) 1. 205
- Fig. 8.3** The normalized pore pressure isochrones (Darcian and non-Darcian) having boundrirs parameters  $R_T=R_B=10$  and  $R_T=R_B=\infty$  at two different times ( $t=2.1 \times 10^8$ sec and  $t=2.2 \times 10^9$ sec) corresponding to different non-Darcian flow parameters: (a)  $a=0.2, \theta=0.5, i_1=45$ ; (b)  $a=0.5, \theta=0.5, i_1=45$ ; (c)  $a=0.8, \theta=0.5, i_1=45$ ; (d)  $a=0.5, \theta=1, i_1=5$ ; (e)  $a=0.5, \theta=0.5, i_1=5$ ; and (f)  $a=0.5, \theta=1, i_1=5$ . 206
- Fig. 8.4** The variation of normalized pore water pressure isochrones (Darcian and non-Darcian) corresponding to four different layer thicknesses ( $h_s=1m, 5m, 10m$ , and  $50m$ ) with  $R_T=R_B=10$  and reported at the same (a) time ( $t=3.5 \times 10^6$  sec) and (b) time-factor ( $T_{vw}=0.02$ ) 207
- Fig. 8.5** The variation of normalized pore water pressure isochrones (Darcian and non-Darcian) at  $t=9.1 \times 10^7$ sec with three different bottom conditions (namely,  $R_B=1, 5$ , and  $10$ ) and two different level of permeability at the top surface: (a)  $R_{Tw}=R_{Ta}=\infty$  and (ii)  $R_{Tw}=R_{Ta}=0$ . 208
- Fig. 8.6** The variation of  $U_{avg}$  versus time (Darcian and non-Darcian) corresponding to one-way, semipermeable ( $R_T=R_B=10$ ), and two-way drainage systems by varying the non-Darcian flow parameters: (a)  $a=0.2, \theta=0.5, i_1=5$ ; (b)  $a=0.5, \theta=0.5, i_1=5$ ; (c)  $a=0.8, \theta=0.5, i_1=5$ ; (d)  $a=0.5, \theta=1, i_1=45$ ; (e)  $a=0.5, \theta=0.5, i_1=45$ ; and (f)  $a=0.5, \theta=1, i_1=45$ . 210

- Fig. 8.7** The variation of  $U_{avg}$  versus time (Darcian and non-Darcian) corresponding to three different semipermeable ( $R_T (=R_B) = 1, 5, \text{ or } 10$ ) drainage systems with  $a=0.2, \theta=0.5, i_1=5$  and permeability ratios ( $k_{ws}=0.01k_{as}$ ) equals to (i) 0.01. (ii)0.1, and (1). 211
- Fig. 8.8** The variation of  $U_{avg}$  versus time (Darcian and non-Darcian) for different semi-permeable bottom layer ( $R_B=1, 10, \text{ and } 100$ ), with  $a=0.2, \theta=0.5, i_{tg}=5, k_{ws}=k_{as}$  and different drainage condition at the top: (a) fully pervious ( $R_T=\infty$ ), and (b) completely impervious ( $R_T=0$ ). 212
- Fig. 8.9** The variation of  $t_{sp}$  with  $R_{Tw}$  and  $R_{Ta}$  considering the ability of air and water flow through the bottom surface to be (a) the same ( $R_B = 10$  or 10000) and (b) different ( $R_{Bw}=100, R_{Ba}=1$  or  $R_{Bw}=10, R_{Ba}=500$ ). 213
- Fig. 8.10** The variation of normalized pore pressures (Darcian and non-Darcian) with time subjected to variable  $R_{Ta} (=1, 5, \text{ and } 100)$  and computed at three different locations (i)  $h/h_s=0.2$ , (ii)  $h/h_s=0.5$ , and (iii)  $h/h_s=0.8$ . 215
- Fig. 8.11** The variation of normalized pore pressures (Darcian and non-Darcian) with time subjected to variable  $R_{Tw} (=1, 5, \text{ and } 100)$  and computed at three different locations (i)  $h/h_s=0.2$ , (ii)  $h/h_s=0.5$ , and (iii)  $h/h_s=0.8$ . 216
- Fig. 8.12** The three-dimensional  $U_{avg}-R_T-R_B$  surfaces drawn at different time (a) view 1 (b) view 2. 218
- Fig. 8.13** The verifications of the present solutions on the basis of: (a) normalized isochrones, (b) pore water pressure profile drawn at  $h/h_s=0.8$ , (c)  $U_{avg,w}$  vs.  $t$  curves corresponding to various  $R_{Tw}$ , and (d)  $U_{avg,a}$  vs.  $t$  curves corresponding to various  $R_{Ta}$ . 219

## LIST OF TABLES

---

---

<b>Table 3.1</b>	A comparison of the present numerical solutions with the analytical solutions presented by Lovisa et al.(2010; 2012).	76
<b>Table 4.1</b>	Specification of the sample	87
<b>Table 4.2</b>	Data used for the analysis	100
<b>Table 4.3</b>	Variation between various cases due to changes in state parameters for ramp loading under PTPB and PTIB conditions	107
<b>Table 4.4</b>	Variation between various cases due to changes in state parameters for constant loading under PTPB and PTIB conditions	108
<b>Table 6.1</b>	The form of the converted algebraic equation corresponding to different method of CNI scheme.	156
<b>Table 6.2</b>	The form of the converted algebraic equation corresponding to different method of BKC scheme.	157
<b>Table 6.3</b>	Stepwise algorithm of CNI and ADE scheme.	158
<b>Table 6.4</b>	The comparison of $u$ from CNI and BKC schemes	161
<b>Table 6.5</b>	A comparison of the present solutions with the solutions computed by Lovisa et al. (2010) and (2012)	167



## LIST OF NOTATIONS

---

<b>Symbol</b>	<b>Definition</b>
$\eta$	Ratio of loading time period and rest time period
$\sigma$	Total stress
$\sigma'$	Effective stress
$\sigma_0'$	Initial effective stress within the soil
$\theta$	Model parameter for non-Darcian flow equation
$\gamma_w$	Unit weight of water
$\Delta t$	Time interval
$\alpha$	Degree of skewness
$\chi$	Angle of arched distributions
$\beta_{aw}$	Compressibility of the air-water mixture
$\beta_w$	Compressibility of the water
$\beta_a$	Compressibility of the air
$\beta$	Variable dependent on $C_c$ and $M$
$A$	Void ratio where effective stress is 1kPa
$a$	Model parameter for non-Darcian flow equation
$b_1, b_2, b_3$ and $b_4$	Geometrical parameter of initial excess pore water pressure distribution
$B$	Void ratio intercept where permeability is 1m/sec
$c_v$	Coefficient of consolidation.
$C_c$	Compression index
$c_v^w$	Coefficient of consolidation for water phase in unsaturated soil
$c_v^a$	Coefficient of consolidation for air phase in unsaturated soil
$D_u$	Range of elastic deformation in $U_{avg}$ curve
$D_s$	Range of elastic deformation in settlement curve
$D_a$	Stress-state independent transmissivity coefficient of the air phase.
$e$	Void ratio of soil
$e_0$	Initial void ratio of soil
$E'$	Exponential hydraulic gradient equation

$E$	Differentiated form of non-darcian velocity
$h_2$	The thickness of the bottom layer in two layerd soil strata
$h_1$	The thickness of the top layer in two layerd soil strata
$H$	Thickness of the soil layer
$h_T$	Thickness of top impeded boundary
$h_B$	Thickness of bottom impeded boundary
$i$	Hydraulic conductivity
$i_1$	Model parameter for non-Darcian flow equation
$J_a$	Mass rate of air
$k$	Vertical permeability of soil layer
$k_j$	Vertical permeability of the $j^{\text{th}}$ layer
$k_1$	Vertical permeability of the top layer in two layerd soil strata
$k_2$	Vertical permeability of the bottom layer in two layerd soil strata
$k_u$	Ultimate permeability
$k_T$	Permeability of top-impeded boundary
$k_B$	Permeability of bottom-impeded boundary
$k_{as}$	Permeability of air phase in soil layer
$k_{ws}$	Permeability of water phase in soil layer
$M$	Slope of $e$ -log $k$ graph
$m_v$	Coefficient of volume compressibility
$m_{v1}$	Coefficient of volume compressibility of the top layer in two layerd soil strata
$m_{v2}$	Coefficient of volume compressibility of the top layer in two layerd soil strata
$m_{1k}^s$	Coefficients of overall volume change with respect to $(\sigma - u_a)$
$m_{1k}^w$	Coefficients of water phase volume change with respect to $(\sigma - u_a)$
$m_{1k}^a$	Coefficients of air phase volume change with respect to $(\sigma - u_a)$
$m_2^s$	Coefficients of overall volume change with respect to $(u_a - u_w)$
$m_2^w$	Coefficients of water phase volume change with respect to $(u_a - u_w)$
$m_2^a$	Coefficients of air phase volume change with respect to $(u_a - u_w)$
$n$	Porosity

$q$	Constant external load
$q_0$	Ultimate load in time-dependent loading
$R_I$	Normalized area of undissipated excess PWP attained at any arbitrary time during consolidation for non-uniform $u_0$ distribution.
$R_0$	Normalized area of undissipated excess PWP attained at any arbitrary time during consolidation for uniform $u_0$ distribution.
$R_T$	Model parameter of top impeded boundary
$R_B$	Model parameter of bottom impeded boundary
$R_{Ta}$	Model parameter of top impeded boundary air phase
$R_{Ba}$	Model parameter of bottom impeded boundary air phase
$R_{Tw}$	Model parameter of top impeded boundary water phase
$R_{Bw}$	Model parameter of bottom impeded boundary air phase
$s^*$	Maximum settlement at load $q_u$
$s$	Settlement of soil at the top surface
$S$	Degree of saturation
$T$	Temperature
$t$	Arbitrary time
$t_0$	Time (1 year)
$t_c$	Construction time
$T_v$	Time factor
$u_0$	Initial excess pore water pressure
$u_{0max}$	Maximum value of initial excess pore water pressure
$u$	Excess pore water pressure
$u_{max}$	Peak position of the isochrones
$U_{avg}$	Average degree of consolidation
$U_z$	Degree of consolidation at any definitive depth
$u_w$	Pore pressure of water phase in unsaturated soil
$u_a$	Pore pressure of air phase in unsaturated soil
$u_{a0}$	Initial excess pore pressure of air phase in unsaturated soil
$u_{w0}$	Initial excess pore pressure of water phase in unsaturated soil
$U_{avga}$	The average degree of consolidation for the air phase
$U_{avgw}$	The average degree of consolidation for the water phase
$V_a$	The volume of free air dissolved air

$V_d$	Volume of free dissolved air
$V_w$	Volume of water
$V_0$	The total volume of soil
$V_v$	Volume of void
$v$	Velocity of water within the soil
$z$	Depth from the top surface
$Z$	Normalised depth with respect to the maximum flow path
$z_l$	The value of $Z$ at the bottom layer

## LIST OF ABBREVIATIONS

---

---

<b>Symbol</b>	<b>Definition</b>
<i>CN</i> method	Crank-Nicolson method
<i>CDK</i>	Constant loading, Darcian flow law and constant permeability
<i>CDKV</i>	Constant loading, Darcian flow law and variable permeability
<i>CNDK</i>	Constant loading, Non-Darcian flow law and constant permeability
<i>CNDKV</i>	Constant loading, Non-Darcian flow law and variable permeability
<i>DF</i>	Darcian flow
<i>NDF</i>	Non-Darcian flow
<i>PWP</i>	Pore water pressure
<i>PTPB</i>	Pervious top pervious bottom
<i>PTPB</i>	Pervious top impervious bottom
<i>RDR</i>	Rate of dissipation ratio
<i>RDK</i>	Ramp loading, Darcian flow law and constant permeability
<i>RDKV</i>	Ramp loading, Darcian flow law and variable permeability
<i>RNDK</i>	Ramp loading, Non-Darcian flow law and constant permeability
<i>RNDKV</i>	Ramp loading, Non-Darcian flow law and variable permeability
<i>RL</i>	Rectangular loading
<i>TL</i>	Trapezoidal loading
<i>TRL</i>	Triangular loading